Semicond. Sci. Technol. 8 (1993) 1465–1469. Printed in the UK

LETTER TO THE EDITOR

Cyclotron resonance of high-mobility GaAs/AlGaAs (311) 2DHGs

S J Hawksworth†, S Hill‡, T J B M Janssen§, J M Chamberlain†, J Singleton‡, U Ekenberg‖, G M Summers‡, G A Davies¶, R J Nicholas‡, E C Valadares†, M Henini† and J A A J Perenboom§

†Department of Physics, University of Nottingham, Nottingham NG7 2RD, UK
‡Clarendon Laboratory, University of Oxford, Oxford OX1 3PU, UK
§High Field Magnet Laboratory, Nijmegen, 6525ED, The Netherlands
‖Royal Institute of Technology, Stockholm, S-10044, Sweden
¶National Pulsed Magnet Laboratory, University of New South Wales, NSW 2033, Australia

Received 13 April 1993, accepted for publication 27 April 1993

Abstract. Cyclotron resonance of high-mobility (up to 300 000 $cm^2 V^{-1} s^{-1}$ at 100 mK) GaAs/AlGaAs two-dimensional hole gases (2DHGS) grown on (311)A oriented substrates has been measured in magnetic fields up to 17 T and at temperatures down to 350 mK. The 2D hole density is in the range (1.0–2.0) $\times 10^{11}$ cm^{-2}. Two resonances are in general observed; at low magnetic fields the lower-field resonance dominates but a progressive transfer of oscillator strength takes place as the field increases. A self-consistent calculation of the Landau fan diagram for the higher-symmetry (100) direction is used to interpret the data and identify the observed transitions.

The key differences between two-dimensional hole gases (2DHGS) and two-dimensional electron gases (2DEGs) are that the former can have much higher effective masses and exhibit greater subband anisotropy. In addition, the electron–phonon interaction in 2DHG systems is rather stronger than in the companion electron gas. Until recently, the general quality of available 2DHG GaAs/AlGaAs material (largely grown on (100) surface substrates) has been rather poor. In consequence, a full exploration of effective masses and valence band anisotropy, using the proven technique of cyclotron resonance (CR) spectroscopy in the far infrared (FIR), has not been possible. A recent development in growth procedures [1] has enabled very high-mobility 2DHG layers to be produced by growth in non-conventional directions (e.g. the (311)A direction) which contain a high ratio of single-to-double dangling bonds with a resultant reduction in carbon and sulphur contaminant incorporation. Using this technique, hole mobilities exceeding 300 000 $cm^2 V^{-1} s^{-1}$ at low temperatures have been achieved in such high-index plane 2DHGs [2], and transport studies [3, 4] in both low- and high-density 2DHG samples have revealed transitions to an insulating state consistent with a magnetically induced Wigner solid.

The valence band structure in GaAs/AlGaAs quantum well (QW) systems exhibits a richness and complexity even for such high-symmetry directions as (100) [5]. For layers grown on the lower-symmetry (311)A direction, magnetotunnelling spectroscopy studies [6] and calculations [7, 8] of valence band anisotropy in quantum wells indicate an even greater degree of mixing, leading to 'camel's back' behaviour of certain valence subbands. A knowledge of hole masses in such QW systems remains of practical importance in view of the dependence of the threshold current required for population inversion in QW lasers on densities of states and therefore effective masses [9].

In the case of 2DHG heterostructure systems, a triangular function may be used to approximate the confining potential, and the absence of inversion symmetry for this potential leads to the lifting of the Kramers' degeneracy for each subband [10]. Several early calculations of subbands and Landau levels for the 2DHG at the GaAs/AlGaAs interface have been reported [11, 12]. The most complete [13] utilizes a fully self-consistent treatment which provides theoretical evidence for strongly nonlinear magnetic field dependence of the Landau-level energies but which does not invoke many-body effects which had been considered important by previous workers. These calculations [13] have been reported only for the high-symmetry (100) direction, and have generally used an axial approximation which introduces a cylindrical

0268-1242/93/071465 + 05 $07.50

symmetry into the 4 × 4 Luttinger Hamiltonian. The extension of these calculations to the lower-symmetry (311)A direction represents a considerable complication, since the axial approximation cannot be made for the lower-symmetry Hamiltonian.

Several early experimental CR studies have been reported for (100)-direction GaAs/AlGaAs 2DHG systems [10, 14, 15]. Although agreement with theory is only partial, these reports demonstrate that strong anisotropy and subband mixing occurs even for the high-symmetry direction, and that the classification into light and heavy holes has lost its meaning. There appears to be only one previous account of an experimental study of CR for the (311) direction [16]; these authors, working with two samples of 2D hole densities 0.8×10^{11} cm^{-2} and 1.8×10^{11} cm^{-2}, find anomalous line splittings in the CR at a magnetic field value which increases with increasing 2D carrier density. This splitting originated, it was suggested, in either an excited-state anticrossing effect or in a many-body effect of a type previously considered for a 2DEG [17].

In this letter, we report an experimental investigation of CR splitting effects in a larger number of samples than hitherto used [16]. Since no theory for the (311)A direction is currently available, the previous calculation [13] for the high-symmetry (100) direction is extended to magnetic fields and 2D hole concentrations appropriate to the present measurements. It is shown that the discontinuity effects noted in the present and previous [16] measurements can be reasonably well accounted for using appropriate CR transitions taken from the Landau fan diagram for the (100) direction; discrepancies between theory and experiment are also discussed in terms of the anticipated changes in theory for the (311) direction.

The electrical characteristics of the samples used are shown in table 1. The samples are all grown by molecular beam epitaxy on (311)A-oriented semi-insulating substrates; both silicon and beryllium are used as dopants. A combination of Fourier transform/fixed magnetic field and FIR laser/swept magnetic field techniques is used to study the transmission of the samples in the Faraday orientation at temperatures down to approximately 350 mK and in magnetic fields up to 17 T. The samples used in this investigation were slightly wedged to avoid spurious interference effects. Particular care was taken in the present study to ensure that the magnetic field was exactly perpendicular to the layer planes.

Figure 1 shows a compendium of cyclotron resonance transmission spectra at several different laser wavelengths for NU704 at 350 mK. A considerable variation of integrated absorption strengths and linewidths is observed as a function of magnetic field for this particular sample. The same general pattern is repeated for the other samples studied by the swept field/FIR laser technique. Particularly noteworthy is the weakness of the CR absorption at 320 μm laser wavelength; this results from the laser energy lying at the centre of the anticrossing region for two Landau levels, as will be discussed later. Figure 2 shows the masses derived from laser measurements of this type for another sample (NU703). It is noted that the mass initially rises steeply with field, but

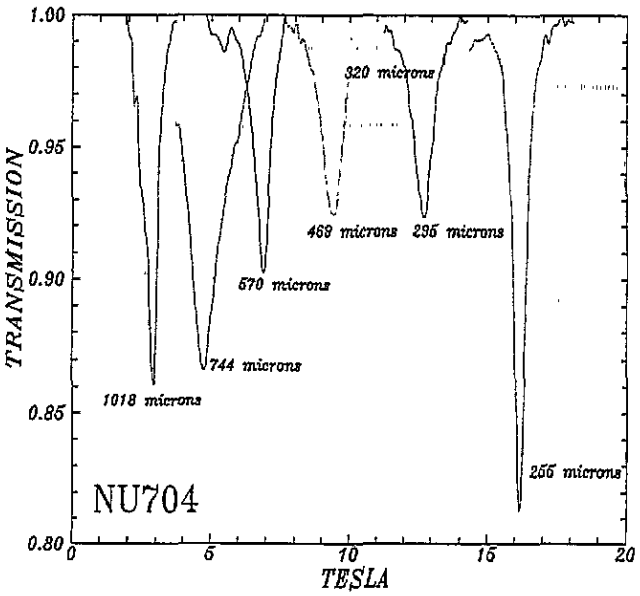

Figure 1. Laser cyclotron resonance spectra for sample NU704 at 350 mK.

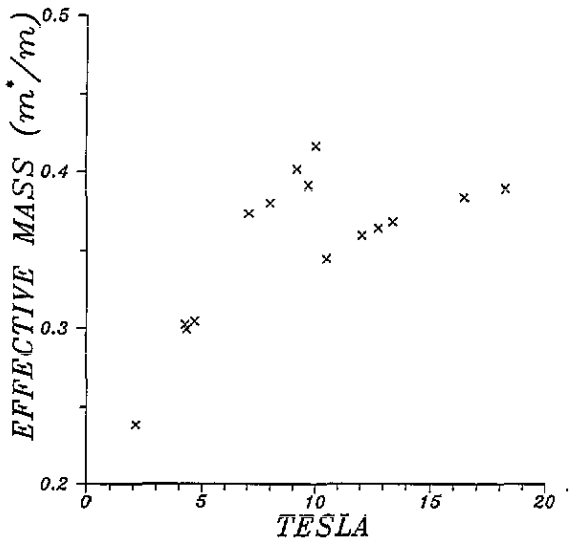

Figure 2. Low-temperature effective masses for sample NU703 obtained from CR absorption spectra.

Table 1. Electrical properties of the samples.

Sample	2D hole concentration (10^{11} cm^{-2})	Approx. 100 mK mobility [4] (cm^2 V^{-1} s^{-1})	Dopant
NU642	1.4		Si
NU703	1.5	300 000	Si
NU704	1.7	300 000	Be
NU738	1.0	150 000	Si
NU740	1.1	150 000	Si
NU811	2.0		Be

that the rise becomes progressively less steep above around 5 T. This behaviour is exhibited for all the samples investigated, as also is the characteristic break in the mass–field curve at the approximate field value for which the absorption strength is minimal.

Figure 3 shows CR data taken in a series of fixed-field/swept frequency experiments for NU704. Similar results are also obtained for the other samples shown in table 1. Two resonances are now generally apparent; the transfer of oscillator strength from the low-field resonance to the high-field resonance is particularly striking. At the lowest fields, there only appears to be one absorption; with increasing magnetic field a smaller absorption feature appears at higher field which grows in strength as the field is increased. The higher-field feature dominates the spectral response at the highest fields investigated, when the low-field feature has virtually disappeared.

Figure 4 shows the magnetic field dependence of the two resonance energies observed for three samples; a shift with areal density of the magnetic field for which the energy splitting of the two resonances is minimal (the 'closest-approach' field) is evident from figure 4. These data are plotted for all samples in figure 5, together with data taken from [16]; a smooth increase in this closest-approach field with rising areal density is noted. Similarly, the mean energy of the two branches at the closest-approach field also displays a linear relationship with sample areal density, as may be seen from figure 6. One of the data points shown in figure 6 is for an experiment in which the sample plane was deliberately tilted 2° from the horizontal; the purpose of this experiment was to demonstrate that the currently observed coupling effects did not originate from a tilted magnetic field [18].

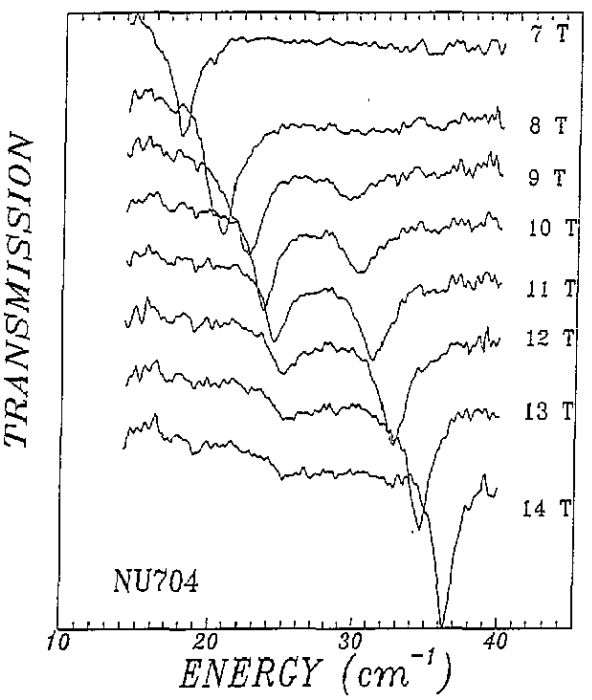

Figure 3. Cyclotron resonance spectra for sample NU704 obtained at 350 mK.

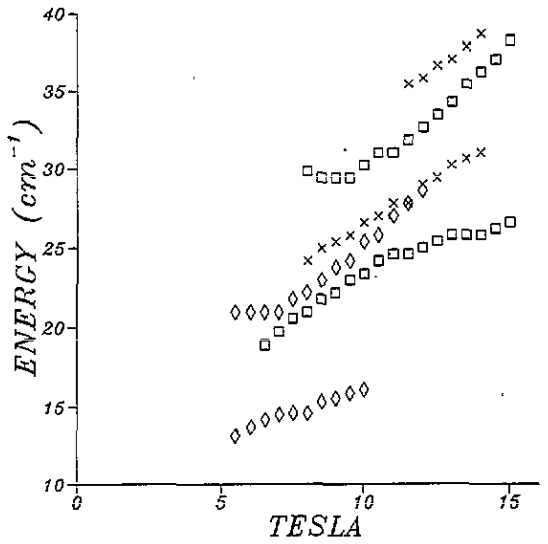

Figure 4. Plot of cyclotron resonance energies and magnetic fields obtained from interferometer data at 350 mK. The symbols represent: □, NU704; ◇, NU738; ×, NU811.

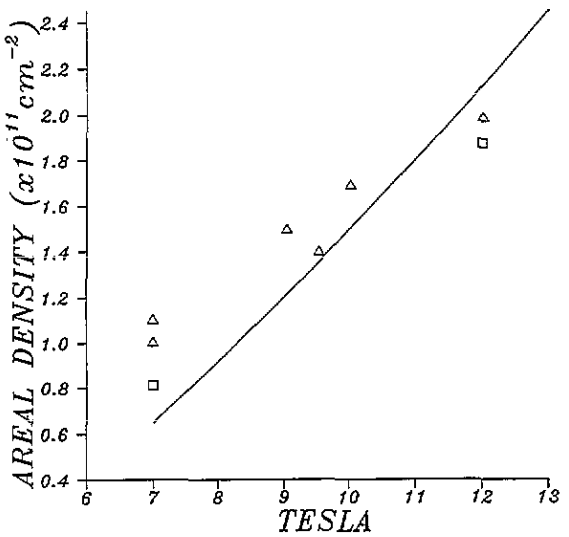

Figure 5. Plot of magnetic field at minimum separation of the branches of the cyclcotron resonance spectra (figure 4) as a function of sample 2D hole density. The symbols are: △, present work; □, data from [16]. The full curve is a plot from theory for the (100) direction (see text).

The self-consistent calculation of Landau fans for the high-symmetry (100) direction [13] has been extended up to 20 T for a range of 2D hole densities between 0.5×10^{11} cm^{-2} and 3.0×10^{11} cm^{-2}. This calculation assumes that the minority donor density in the GaAs region of the heterostructure is 5×10^{14} cm^{-2}. Figures 7(*a*) and (*b*) show the results of this calculation for the limiting values of hole density. The axial approximation used for this direction of symmetry implies that each component of the hole multicomponent wavefunction corresponds to a single Landau level index. The notation used to describe the Landau fans in figures 7(*a*) and 7(*b*) is (m, n), where m is the zero-field subband index and n

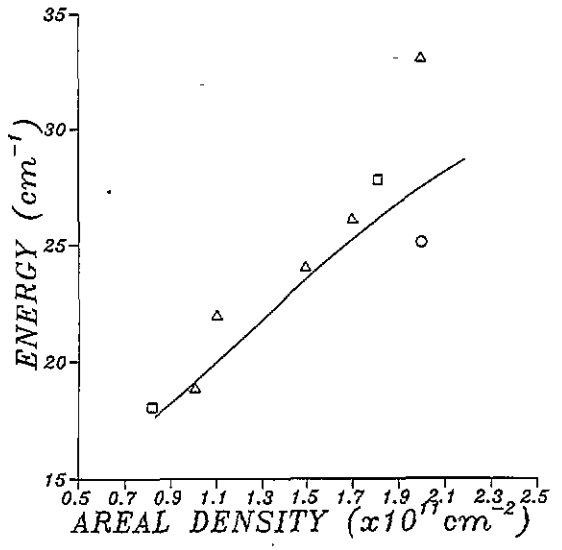

Figure 6. Plot of the mean energy at minimum separation of the branches of the cyclotron resonance spectra (figure 4) as a function of sample 2D hole density. The symbols are: △, present work; □, data from [16]; ○, data for NU811 taken with the magnetic field at 2° to the perpendicular. The full curve is a plot from theory for the (100) direction (see text).

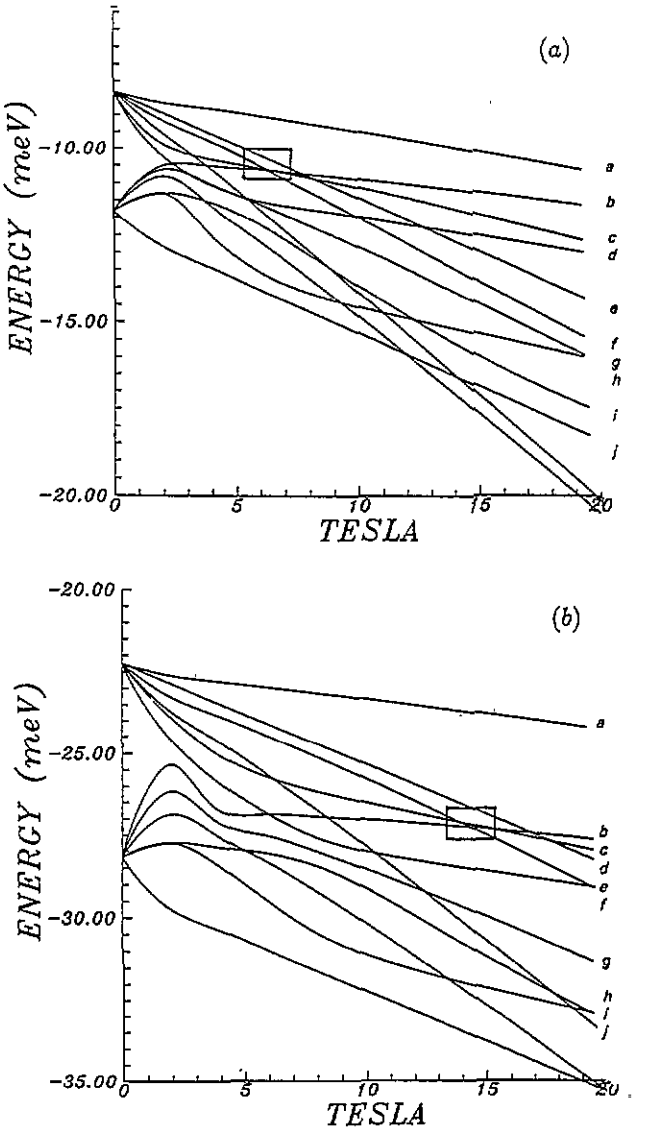

Figure 7. Calculations of the Landau fans for (100) hole gases. (*a*) 2D hole density 0.5×10^{11} cm^{-2}. The ordering of the Landau levels is: a (1, 1); b (2, 1); c (1, $\bar{1}$); d (1, 0); e (1, $\bar{2}$); f (1, 2); g (2, 2); h (2, $\bar{1}$); i (2, 0); j (2, $\bar{2}$). (*b*) 2D hole density 3×10^{11} cm^{-2}. The ordering of the Landau levels is: a (1, 1); b (2, 1); c (1, $\bar{1}$); d (1, $\bar{2}$); e (1, 0); f (1, 2); g (2, 2); h (2, 0); i (2, $\bar{1}$); j (1, 3).

the Landau index for that subband (negative spin states are designated thus: $\bar{n}$). At zero field only, the $m = 1$ state corresponds to the HH1 and $m = 2$ to the LH1 states. It is evident from figures 7(*a*) and 7(*b*) that the zero-field subband separation reduces with reducing areal density; this behaviour might also be expected from a simple triangular model for the 2DHG heterostructure potential [19]. It is also evident from these figures that the Landau level fans exhibit strong non-parabolicity and that many level-crossings may be observed. At finite values of magnetic field, the crossings observed in the fan diagram occur at progressively higher magnetic fields as the areal density increases; this is illustrated for a particular crossing by a 'box' in the two figures. This behaviour follows from the fact that the interaction between the corresponding Landau levels decreases as the areal density increases, and thus an enhancement of their interaction can only be achieved at higher fields.

Additional evidence for the strong interaction between Landau levels is provided by the effective-mass curves of figure 2 for the stronger cyclotron absorption. At low fields the heavy hole exhibits a relatively low mass but this mass increases with field, owing to coupling within the Luttinger Hamiltonian [20]. The curve displays the discontinuity at the closest-approach field, as might be expected, but above this field the mass curve increases less steeply, which might be construed as evidence for increased subband decoupling effects within the Hamiltonian.

The origin of the two resonances will now be discussed using the calculated Landau fans for the (100) direction for illustration. For the present samples, transport measurements [3] indicate that the extreme quantum limit is achieved at magnetic fields of 5–6 T. CR transitions will occur from the (1, 1) ground state and will be governed by appropriate selection rules. Although no calculation of these selection rules for the lower-symmetry (311) direction has yet been undertaken, it seems likely that transitions within the same subband manifold will have a greater oscillator strength and that transitions for which the symmetry changes will also be less favoured. Appropriate candidates for the two transitions noted in figure 3 are therefore (1, 1) → (1, 2) and (1, 1) → (2, 1) for the stronger and weaker lines respectively. A consideration of the ordering of the states and the spin-flip transition rule leads to a rejection of the transitions (1, 1) → (1, $\bar{2}$) and (1, 1) → (1, $\bar{1}$).

Additional evidence for the mechanism suggested above is provided by the general agreement between experimental data and theory shown in figures 5 and 6. In

the case of a coupling in a 2DEG induced by a tilted magnetic field [21], a plot of the type shown in figure 6 yields the zero-field subband separation. This is not the case for the complicated valence band structure in 2DHGs, since the (2, 1) and (1, 1) levels do not remain parallel as the field changes. Nevertheless, the energy values plotted in figure 6 do represent the energy between the ground (1, 1) state and the energy at the closest-approach field, which may be compared with theory for different density samples using the crossing highlighted by a box in figure 7.

In conclusion, we have measured the CR behaviour of several high-mobility 2DHG samples grown on [311]-oriented planes in magnetic fields up to 17 T. Using swept-frequency/fixed-field spectroscopy two resonances are generally observable at a given field; the absorption strength shifts from the lower-field to the higher-field resonance as magnetic field increases. A Landau fan diagram calculation for the (311) direction is extremely difficult, due to the problem of establishing an appropriate ansatz for solving the Hamiltonian in this low-symmetry direction. The present data have therefore been compared with self-consistent theory for the higher-symmetry (100) direction, assuming that the observed absorptions represent the $(1, 1) \rightarrow (1, 2)$ and $(1, 1) \rightarrow (2, 1)$ transitions. In general, these calculations provide strong support for the proposed mechanism. For the lower-symmetry (311) direction, additional off-diagonal terms will appear in the Hamiltonian, leading to even greater mixing effects (so that many of the crossings shown in figure 7 will become anticrossings) and further relaxation of selection rules for CR transitions may also occur.

Acknowledgments

The samples were grown as part of the NUMBERS project at Nottingham University, which is funded by the Science and Engineering Research Council (SERC) in the UK. The use of the High Magnet Field Laboratory at KU, Nijmegen is made possible by an EEC Large Installations grant and general support from the Stichting voor Fundamenteel Onderzoek der Materie (FOM) in The Netherlands. SJH records his gratitude to GMMT Ltd for a CASE award. Several useful discussions with B L Gallagher are acknowledged. The assistance of R T Grimes with some parts of the data analysis is also acknowledged.

References

[1] Wang W I, Mendez E E, Iye Y, Lee B, Kim M H and Stillman G E 1986 *J. Appl. Phys.* **60** 1834
[2] Davies A G, Frost J E F, Ritchie D A, Peacock D C, Newbury R, Lindfield E H, Pepper M and Jones G A C 1991 *J. Crystal Growth* **111** 318
[3] Santos M B, Suen Y W, Shayegan M, Li Y P, Engel L W and Tsui D C 1992 *Phys. Rev. Lett.* **68** 1188
[4] Rodgers P J, Langerak C J G M, Gallagher B L, Barraclough R J, Henini M, Foster T J, Hill G, Wiegers S A J and Perenboom J A A J 1993 *Physica* B **184** 95
[5] Hayden R K, Maude D K, Eaves L, Valadares E C, Henini M, Sheard F W, Hughes O H, Portal J C and Cury L 1991 *Phys. Rev. Lett.* **66** 1749
[6] Harrison P A, Hayden R K, Henini M, Valadares E C, Hughes O H and Eaves L 1992 *J. Vac. Sci. Technol.* B **10** 2040
[7] Valadares E C 1992 *Phys. Rev.* B **46** 3935
[8] Ikonic Z, Milanovic V and Tjapkin D 1992 *Phys. Rev.* B **46** 4285
[9] Meney A T 1992 *Superlatt. Microstruct.* **11** 31
[10] Stormer H L, Schlesinger Z, Chang A, Tsui D C, Gossard A C and Wiegmann W 1983 *Phys. Rev. Lett.* **51** 126
[11] Ando T 1985 *J. Phys. Soc. Japan* **54** 1528
[12] Broido D A and Sham L J 1985 *Phys. Rev.* B **31** 888
[13] Ekenberg U and Altarelli M 1985 *Phys. Rev.* B **32** 3712
[14] Bangert E and Landwehr G 1986 *Surf. Sci.* **170** 593
[15] Schlesinger Z, Allen S J, Yafet Y, Gossard A C and Wiegmann W 1985 *Phys. Rev.* B **32** 5231
[16] Schlesinger Z and Wang W I 1986 *Phys. Rev.* B **33** 8867
[17] Schlesinger Z, Allen S J, Hwang J C M, Platzman P M and Tsoar R 1984 *Phys. Rev.* B **30** 435
[18] Stanaway M B, Langerak C J G M, Thomeer R A J, Chamberlain J M, Singleton J, Henini M, Hughes O H, Page A J and Hill G 1991 *Semicond. Sci. Technol.* **6** 208
[19] Ando T, Fowler A B and Stern F 1982 *Rev. Mod. Phys.* **54** 437
[20] Plaut A S, Singleton J, Nicholas R J, Harley R T, Andrews S R and Foxon C T B 1988 *Phys. Rev.* B **38** 1323
[21] Sigg H, Langerak C J G M and Perenboom J A A J 1987 *High Magnetic Fields in Semiconductor Physics* (*Springer Series in Solid State Science 71*) ed G Landwehr p 248